Bulgarian Chemical Communications, Volume 56, Issue 2 (pp. 107-124) 2024 *DOI: 10.34049/bcc.56.2.5625*

Synthesis, biological evaluation, ADME studies and molecular docking with β-tubulin of fused benzimidazole-pyridine derivatives

D. Panchani[1], S. Maurya[1], T. Thaker[1]*, V. Rathod[1], Sh. Thakur[2]

[1]*Department of Chemistry, Parul Institute of Applied Sciences, Parul University, Waghodia, Vadodara-391760, Gujarat, India*

[2]*Department of Forensic Science, Parul Institute of Applied Sciences, Parul University, Waghodia, Vadodara-391760, Gujarat, India*

Received January 25, 2024; Revised: May 21, 2024

After treatment with chloroacetyl chloride, 2-(pyridin-4-yl)-1H-benzo[d]imidazole underwent a reaction to yield 2-chloro-1-(2-(pyridin-4-yl)-1H-benzo[d]imidazol-1-yl) ethan-1-one. The latter intermediately reacted with one equivalent of various primary aromatic amines in the presence of potassium carbonate in chloroform, yielding the respective target amine derivatives of benzimidazole. The structure of the synthesized compounds was established by ^{1}H NMR, IR, and mass spectrometry. Synthesized compounds were screened for antimicrobial activity by diffusion plate method and most of them showed moderate to good potency against *Staphylococcus aureus, Bacillus subtilis, Escherichia coli,* and *Pseudomonas aeruginosa.* Compound *3a* showed the best potency compared to others. To predict the pharmacokinetics and drug-like properties of the synthesized substances, absorption, distribution, metabolism, and excretion (ADME) models were employed. Computational methods, along with a set of criteria based on Lipinski and Veber rules, were utilized to anticipate the physicochemical features indicative of drug-likeness for the synthesized molecules. Furthermore, molecular docking tests against 1SA0 (β-tubulin) were conducted, and the results demonstrated favorable interactions of the compounds with the target, with binding energy values approaching 5Å.

Keywords: Benzimidazole, Molecular docking, β-Tubulin, Antibacterial activity.

INTRODUCTION

The investigation of the biological dynamics of targeted benzimidazoles with β-tubulins through molecular docking and simulations in the context of anthelmintic action is intriguing. Microtubules (MT) are protein polymers characterized by tubular structures composed of tubulin subunits, playing a crucial role in the cell's cytoskeleton. They are essential for maintaining cell shape, facilitating intracellular material movement, and executing mitosis. Additionally, they are integral components connected to the mitotic spindle, centrioles, microtubules, cilia, and flagella [1].

Benzimidazole, featuring a benzene ring fused with imidazole, exhibits a delicate structure and versatile therapeutic benefits. An illustrative example of benzimidazole is cyanocobalamin vitamin [2]. Due to their inhibitory activity and favorable selectivity ratio, benzimidazoles demonstrate significant medicinal potency. Various biochemical and pharmaceutical investigations have highlighted the efficacy of benzimidazole compounds against diverse bacteria [3]. These compounds exhibit antioxidant, antiproliferative [4], anthelminthic, antihypertensive [5], anti-inflammatory, antiparasitic, antineoplastic [6], antiprotozoal [7], anti-HIV [8], and anti-trichinellosis [9] actions, showcasing the versatility of this ring system [10]. The popular medications lansoprazole and esomeprazole contain two heterocyclic moieties, pyridine and benzimidazole [11]. Retinoidal monocationic benzimidazole molecule bears the most potent antimicrobial activity [12]. Moreover, the presence of certain organic groups, such as amino, nitro, hydroxy, methoxy, sulfamide, carboxylic acid, etc., increase the biological activities of the compounds [13],

Consequently, the current study aims to synthesize and evaluate the biological activities of newly derived benzimidazole-pyridine moieties. The synthesized moieties were characterized through various spectroscopic studies. Subsequent ADME studies and molecular docking of novel analog s using beta-tubulin (PDB-1SA0) were undertaken to further elucidate their potential.

MATERİALS AND METHODS

General information

All chemicals were procured from Sigma Aldrich. The solvents used were of analytical reagent (AR) grade. Melting points were determined

* To whom all correspondence should be sent:
E-mail: tirth6582@gmail.com

using the Equiptronics model EQ-730 instrument. The reaction was monitored by thin layer chromatography (TLC) and was carried out on Merck silica gel 60 F_{254} plates. Visualization of the plates was done using a UV lamp (λ_{max} = 254 or 365 nm). The IR spectra were recorded using KBr pellets on Bruker alpha-II FTIR spectrometer. Deuterated solvents (DMSO-d_6) were utilized for capturing ^{1}H NMR spectra on Bruker 400 MHz spectrometer, with tetramethyl silane serving as the internal standard. Mass spectral data were recorded using a Shimadzu LC2010 mass analyzer, and elemental analysis revealed that values were consistent within 0.4% of their theoretical counterparts. C, H, N analyses was conducted using a Perkin Elmer PE 2400.

- *General synthesis of 2-(pyridin-4-yl)-1H-benzo[d]imidazole [compound 1]*

Ortho-phenyl diamine (3 g, 0.0027 moles) and isonicotinic acid (3.41 g, 0.0027 moles) were dissolved in ortho-phosphoric acid (20 ml) and stirred for 24 hours at 130-140°C until the starting material was completely consumed. Subsequently, the mixture was cooled in an ice bath, and pH was maintained at 8-9 by adding 20% NaOH. The resulting precipitate was separated through filtration, washed with methanol, and the solvent was subsequently evaporated.

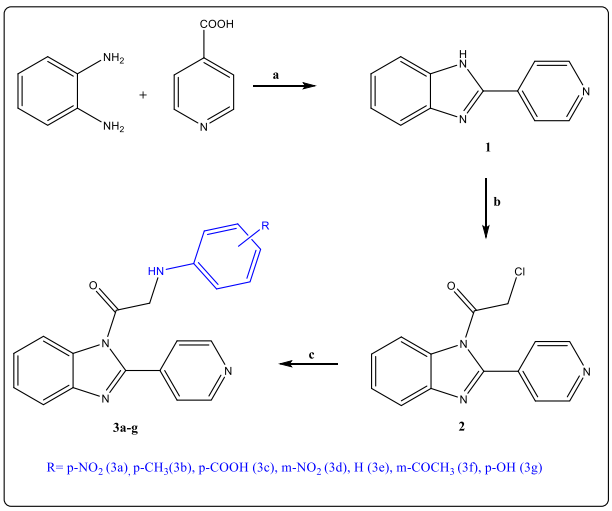

Scheme 1. Reagent and conditions of benzimidazole with pyridine moiety synthesis: (a) ortho-phosphoric acid, 130-140°C, reflux for 24 h; (b) chloroacetyl chloride, diethyl ether, at room temperature, stirred for 24 h; (c) potassium carbonate, chloroform, at 40-50°C and reflux for 12 h.

Yield: 89.88 %; M.P: 208-210 °C; Rf: 0.50; IR (Bruker) ν max cm^{-1}: 3054.28(m) (N-H Str.), 1607.86 (C=N Str.), 1430.85 (C=C Str.), 1315.31 (C-N Str. aromatic), 1232.30 (C-H o-substituted Bend), 838.16, 742.39; ^{1}H NMR (DMSO-d_6, 400 MHz): d = 6.67 (m, 2H, J = 8.4 Hz), 7.10 (d, 2H, J = 8.8 Hz), 7.48 (d, 2H, J = 8.0 Hz), 7.88 (d, 2H, J = 8.4 Hz), 12.56 (s, 1H, -NH); MS (m/z): 196.40; $C_{12}H_9N_3$ requires 195.08 Anal. calc. for C, 73.83; H, 4.65; N, 21.52; Found C, 72.98; H, 5.03; N, 21.99.

- *General synthesis of 2-chloro-1-(2-(pyridin-4-yl)-1H-benzo[d]imidazol-1-yl)ethan-1-one [compound 2]*

2-(pyridin-4-yl)-1H-benzo[d]imidazole (1 gm, 0.0051 moles) dissolve in diethyl ether (10 ml) and stir spend half an hour in an ice bath, then the addition of chloroacetyl chloride (2 ml, 0.001 moles) dropwise via syringe at 0°C (ice) and stirred for 24 h and ppt separated via filtration and dry the product and recrystallized using ethanol.

Yield: 88.23%; M.P: 219-225°C; Rf: 0.69; IR (Bruker) ν max cm^{-1}: 1699.25 (C=O str. Imine amide), 1455.21 (CH_2 str.), 1323.20 (C-N str. Aromatic), 1227.57 (C-H O-disubstituted Bend), 878.59, 758.84, 677.47 (C-Cl str.); ^{1}H NMR (DMSO-d_6, 400 MHz): d = 4.12 (s, 2H, CO-$\underline{CH_2}$-Cl), 7.25 (m, 2H, J = 9.2, 3.2 Hz), 7.65 (d, 2H, J = 8.8 Hz), 8.10 (d, 2H, J = 5.6 Hz), 8.75 (d, 2H, J = 5.6 Hz); MS (m/z): 272.80; $C_{14}H_{10}ClN_3O$ requires 271.70. Anal. calc. for C, 61.89; H, 3.71; N, 15.47; Found C, 61.72; H, 3.02; N, 15.80.

- *General synthesis of 2-((R-substituted phenyl)amino)-1-(2-(pyridin-4-yl)-1H-benzo[d] imidazol-1-yl)ethan-1-one [compounds 3a-g]*

A mixture comprising 2-chloro-1-(2-(pyridin-4-yl)-1H-benzo[d]imidazol-1-yl)ethan-1-one (1 gm, 0.0036 moles), substituted amines (p-nitroaniline, p-toluidine, p-aminobenzoic acid, m-nitroaniline, aniline, p-aminoacetophenone, p-aminophenol) (0.0036 moles), and potassium dichromate (0.49 gm, 0.0036 moles) in 10 ml chloroform at reflux and continuous stirring for 12 hours. The reaction progress was monitored using TLC. Upon completion, the reaction mixture was filtered, and the solvents were evaporated. The resulting product was then dried and subjected to recrystallization in ethanol.

- *2-((4-nitrophenyl)amino)-1-(2-(pyridin-4-yl)-1H-benzo[d]imidazol-1-yl)ethan-1-one [3a]*

Yield: 68.13%; M.P: 290-291°C; Rf: 0.30; IR (Bruker) ν max cm^{-1}: 3354.14(m) (N-H str.), 1641.50 (C=O str. Imine amide), 1629.54 (C=N), 1585.05 (N=O str.), 1470.61 (CH_2 str.), 1315.31 (N=O str.), 1296.86, 1111.08, 838.00 (C-H bend p-disubstituted), 751.21 (C-H O-disubstituted); ^{1}HNMR (DMSO-d_6, 400 MHz): d = 5.63 (s, 2H, CO-$\underline{CH_2}$-NH), 6.60 (d, 2H, J = 9.2 Hz), 7.37 (d, 2H, J = 9.2 Hz), 7.42 (s, 1H, CO-CH_2-$\underline{NH}$), 7.74 (m, 2H, J = 9.2, 3.2 Hz), 7.91 (d, 2H, J = 9.2 Hz), 8.66 (d, 2H, J = 6.0 Hz), 9.01 (d, 2H, J = 6.4 Hz); MS (m/z):

374.54 $C_{20}H_{15}N_5O_3$ requires 373.37. Anal. calc. for C, 64.34; H, 4.05; N, 18.76; Found C, 64.72; H, 4.95; N, 17.96.

- *1-(2-(pyridin-4-yl)-1H-benzo[d]imidazol-1-yl)-2-(p-tolylamino)ethan-1-one [3b]*

Yield: 65%; M.P: 201-203°C; Rf: 0.27; IR (Bruker) ν max cm^{-1}: 3333.40(m) (N-H str.), 3054 (CH_3 str.), 1607.86 (C=O str. Imine amide), 1430.98 (C=C str.), 1314.73 (CH_3 str.), 1232.30, 998.11, 838.53 (C-H bend p-disubstituted), 742.87 (C-H bend o-disubstituted); ^{1}H NMR (DMSO-d_6, 400 MHz): d = 2.11 (s, 3H, Ar-$\underline{CH_3}$), 4.79 (s, 2H, CO-$\underline{CH_2}$-NH), 6.46 (s, 1H, CO-$CH_2\underline{NH}$), 6.82 (d, 2H, J = 8.0 Hz), 7.25 (m, 4H, J = 4.0, 7.2 Hz), 7.66 (m, 2H, J = 9.2, 3.2 Hz), 8.10 (d, 2H, J = 6.0 Hz), 8.76 (d, 2H, J = 8.8 Hz); MS (m/z): 343.53 $C_{21}H_{18}N_4O$ requires 342.40. Anal. calc. for C, 73.67; H, 5.30; N, 16.36; Found C, 73.05; H, 5.35; N,17.05.

- *4-((2-oxo-2-(2-(pyridin-4-yl)-1H-benzo[d] imidazol-1-yl)ethyl)amino) benzoic acid [3c]*

Yield: 72.03%; M.P: 143-150°C; Rf: 0.58; IR (Bruker) ν max cm^{-1}: 3380 (N-H str.), 1641.49 (C=O str. Imine amide), 1615.93 (C=O str. Ar-COOH), 1607.86 (C=N str.), 1431.44 (CH_2 bend), 1315.31 (C-N str. aromatic), 1283.09, 1170.20, 834.35 (C-H bend p-disubstituted), 740.23 (C-H O-disubstituted); ^{1}H NMR (DMSO-d_6, 400 MHz): d= 4.33 (s, 2H, CO-$\underline{CH_2}$-NH), 5.87 (s, 1H, CO-CH_2-$\underline{NH}$), 6.58 (d, 2H, J = 9.2 Hz), 7.30 (m, 2H, J = 9.2, 3.2 Hz), 7.64 (d, 2H, J = 12.0, 3.2 Hz), 7.70 (d, 2H, J = 7.2 Hz), 7.77 (d, 2H, J = 6.0 Hz), 8.74 (d, 2H, J = 6.0 Hz), 10.6 (s, 1H, COOH); MS (m/z): 373.12 $C_{21}H_{16}N_4O_3$ requires 372.38. Anal. calc. for C, 67.73; H, 4.33; N, 15.05; Found C, 68.15; H, 4.02; N, 15.76.

- *2-((3-nitrophenyl)amino)-1-(2-(pyridin-4-yl)-1H-benzo[d]imidazol-1-yl)ethan-1-one [3d]*

Yield: 96.06%; M.P: 65-72°C; Rf: 0.33; IR (Bruker) ν max cm^{-1}: 3330.70(m) (N-H str.), 1612.72 (C=O str.), 1519.60 (N=O str.), 1364.75 (CH_2 str.), 1315.31 (C-N str. aromatic), 1072.44, 829.46 (C-H bend p-disubstituted), 735.13 (C-H o-disubstituted); ^{1}H NMR (DMSO-d_6, 400 MHz): d= 4.25 (s, 2H, CO-$\underline{CH_2}$-NH), 5.85 (s, 1H, CO-$CH_2\underline{NH}$), 6.96 (m, 2H, J = 7.6, 1.2 Hz), 7.22 (d, 1H, J = 6.4 Hz), 7.26 (t, 1H, J = 8.8, 1.6 Hz), 7.31 (d, 1H, J = 8.0 Hz), 7.59 (s, 1H), 7.69 (d, 2H, J = 9.2 Hz), 8.19 (d, 2H, J = 6.4 Hz), 8.82 (d, 2H, J = 6.0 Hz); MS (m/z): 374.54; $C_{20}H_{15}N_5O_3$ requires 373.37. Anal. calc. for C, 64.34; H, 4.05; N, 18.76; Found C, 64.12; H, 4.16; N, 18.51.

- *2-(phenylamino)-1-(2-(pyridin-4-yl)-1H-benzo[d]imidazol-1-yl)ethan-1-one [3e]*

Yield: 67.79%; M.P: 202-206°C; Rf: 0.44; IR (Bruker) ν max cm^{-1}: 3365.84(m) (N-H str.), 1610.32 (C=O str. Imine amide), 1576.67 (C=N Str.), 1504.21 (C=C Str.) 1393.17 (C-N str. aromatic), 1314.87 (N=O str.), 1233.29, 745.82 (C-H O-disubstituted), 696.59 (C=C str. Mono substituted); ^{1}H NMR (DMSO-d_6, 400 MHz): d= 5.08 (s, 2H, CO-$\underline{CH_2}$-NH), 6.41 (t, 1H, CO-CH_2-$\underline{NH}$), 6.47 (d, 2H, J = 7.2 Hz), 6.61 (t, 1H, J = 8.4 Hz), 6.99 (m, 2H, J = 10.4, 2.8 Hz), 7.09 (m, 2H, J = 8.8, 2.8 Hz), 7.58 (d, 2H, J = 8.8 Hz), 8.16 (d, 2H, J = 5.6 Hz), 8.65 (d, 2H, J = 6.0 Hz); MS (m/z): 329.25 $C_{20}H_{16}N_4O$ requires 328.48. Anal. calc. for C, 73.15; H, 4.91; N, 17.06; Found C, 73.10; H, 4.12; N, 17.91.

- *2-((3-acetylphenyl)amino)-1-(2-(pyridin-4-yl)-1H-benzo[d]imidazol-1-yl)ethan-1-one [3f]*

Yield: 72%; M.P: 112-115°C; Rf: 0.49; IR (Bruker) ν max cm^{-1}: 3464.76(m) (N-H str.), 3367.05 (C-H str.), 1641.04 (C=O str. Imine amide), 1595.86 (C=N str.), 1490.56 (C=C str.), 1430.85 (N=O str.), 1355.09 (CH_3 bend), 1319.39 (C-N str. aromatic), 1236.42, 1072.60, 868.73 (C-H bend m-disubstituted), 736.77 (C-H o-disubstituted); ^{1}HNMR (DMSO-d_6, 400 MHz): d= 3.31 (s, 3H, CO-$\underline{CH_3}$), 5.32 (s, 2H, CO-$\underline{CH_2}$-NH), 6.80 (m, 2H, J = 7.0 Hz), 7.09 (t, 1H, CO-$\underline{CH_2}$-NH), 7.10 (d, 1H, J = 6.0 Hz), 7.12 (t, 1H, J = 6.6 Hz), 7.16 (d, 1H, J = 6.4 Hz), 7.51 (s, 1H), 8.11 (d, 2H, J = 1.2 Hz), 8.32 (d, 2H), 8.66 (d, 2H, J = 7.2 Hz); MS (m/z): 371.12 $C_{22}H_{18}N_4O_2$ requires 370.41. Anal. calc. for C, 71.34; H, 4.90; N, 15.13; Found C, 71.12; H, 4.71; N, 15.97.

- *2-((4-hydroxyphenyl)amino)-1-(2-(pyridin-4-yl)-1H-benzo[d]imidazol-1-yl)ethan-1-one [3g]*

Yield: 88.60%; M.P: 135-137°C; Rf: 0.80; IR (Bruker) ν max cm^{-1}: 3500-3200(m) (O-H str.), 3278.94 (N-H stretch), 1609.89 (C=O str. Imine amide), 1576.82 (C=N str.), 1508.24 (C=C str.) 1372.01 (C-N str. aromatic), 1233.41, 1003.52, 826.45 (C-H bend p-disubstituted), 741.79 (C-H O-disubstituted); ^{1}HNMR (DMSO-d_6, 400 MHz): d= 4.23 (s, 2H, CO-$\underline{CH_2}$-NH), 6.43 (d, 2H, J = 7.7 Hz), 6.48 (d, 2H, J = 8.0 Hz), 6.70 (s, 1H, CO-CH_2-$\underline{NH}$), 7.26 (m, 2H, J = 7.2, 2.2 Hz), 7.68 (m, 2H, J = 7.6, 2.8 Hz), 8.17 (d, 2H, J = 7.2 Hz), 8.74 (d, 2H, J = 7.2 Hz), 9.98 (s, 1H, Ar-$\underline{OH}$); MS (m/z): 345.41 $C_{20}H_{16}N_4O_2$ requires 344.13; Anal. calc. for C, 69.76; H, 4.68; N, 16.27; Found C, 69.24; H, 4.70; N, 16.31.

Biological evaluation

- *In vitro antibacterial activity*

Synthesized compounds were screened for their antimicrobial activity by using the diffusion plate method. A HiMedia blank disc saturated with a measured quantity (25 µL) of the sample (5 mM) was placed on a plate (9 cm diameter) containing a solid bacterial medium. The incubation period was 24 h at 37 °C, diameter of the zone of inhibition was measured and showed promising inhibitory power of

the sample against bacterial strains [14]. The title compound's antibacterial efficacy was screened against two Gram-positive bacteria (*Bacillus subtilis*, MTCC 441 and *Staphylococcus aureus*, MTCC 96) and two Gram-negative bacteria (*Pseudomonas aeruginosa*, MTCC 1866, and *Escherichia coli*, MTCC 443). Penicillin G was employed as the standard drug procured from HiMedia.

- *In silico study*

The title compound was subjected to an *in silico* study using the SwissADME software [15]. Nocodazole was employed as a reference standard.

- *Molecular docking*

The molecular modeling studies were performed with Discovery studio2021. The RCSB Protein Data Bank (http://www.rcsb.org/pdb) was used to retrieve the X-ray crystallographic structure of the beta-tubulin [16] complex with DAMA-colchicine (PDB: 1SA0). Protein preparation was carried out in AutoDockTools-1.5.6 where standardization of atoms, insertion of missing atoms in the residue, removal of water, addition of polar hydrogen, and addition of Kolman charge were carried out. The nocodazole and 1, 2, 3a-g were drawn through Chemdraw 20.0 and fully minimized and docked using PyRx-Virtual screening tools. Nocodazole is an antiproliferative agent used as a standard, as both tubulin and nocodazole are used to inhibit cell growth.

RESULTS AND DİSCUSSİON

Chemistry

O-phenylene diamine and isonicotinic acid were condensed by dissolving in orthophosphoric acid and refluxed for 24 h at 130-140°C to get 2-(pyridin-4-yl)-1H-benzo[d]imidazole (1). Crude product was purified by recrystallization and maroon solid was obtained with 89.88% yield. The IR spectrum of (1) showed -NH (2°amines) at 3054 cm^{-1}, -C=N of benzimidazole at 1607 cm^{-1}, and C-N of pyridine at 1315 cm^{-1}. ^1H NMR of (1) indicated peak confirmative signals of upfield benzimidazole aromatic protons at 6.67-7.10 ppm, downfield aromatic protons of pyridine at 7.48-7.86 ppm and NH proton at 12.56 ppm. Compound (1) was treated with chloroacetyl dissolved in diethyl ether at 0°C for 24 h to obtain 2-chloro-1-(2-(pyridine-4-yl)-1H-benzo(d]imidazolyl-1-yl) ethan-1-one (2) as green solid with 88.23% yield. IR spectrum of (2) showed disappearance of -NH- (2°amines) peak at 3054 cm^{-1} of compound (1) and appearance of C=O at 1699.25 cm^{-1}, CH_2 at 1455 cm^{-1}, C-Cl at 878.59, 819.33, 758.84 and 677.47 cm^{-1}. ^1H NMR of (2) indicated a CH_2 signal at 4.12 ppm (s); benzimidazole aromatic protons at 7.25-7.65 ppm and pyridine protons at 8.10-8.75 ppm. The disappearance of -NH peak at 12.56 ppm of compound (1) confirms the synthesis. Title compounds 3a-g were synthesized by condensation of (2) with aromatic amines in chloroform at reflux over potassium carbonate for 24 h. Reaction was monitored by TLC. RM was filtered, the solvent evaporated and the crude product was recrystallized in ethanol to yield 65-96% of compounds 3a-g. IR of 3a showed -NH at 3354 cm^{-1}; C=O at 1641 cm^{-1}, C=N at 1629 cm^{-1}, N=O at 1585 cm^{-1}, CH_2 at 1477 cm^{-1}; ^1H NMR showed 3a peaks at 5.63 ppm for O=C-CH_2- group, aromatic protons of p-nitroaniline appeared at 6.60-7.37 ppm, aromatic protons of benzimidazole at 7.74- 7.91 ppm and aromatic protons of pyridine appeared at 8.66-9.01 ppm, NH proton at 7.42 confirmed the synthesis. IR spectrum of 3b showed CH_3 at 1314.73 cm^{-1}, 2° NH at 3333.40 cm^{-1}, C=O at 1607.14 cm^{-1}; ^1H NMR spectrum of 3b indicated CH_3 at 2.11 ppm; O=C-CH_2 at 4.79, ppm -NH at 6.64 ppm all aromatic protons are observed at 6.82-8.76 ppm; IR spectrum of 3c showed -C=O at 1615.93 cm^{-1}, CH_2 at 1431.44 cm^{-1}, -NH at 3380 cm^{-1}. ^1H NMR spectrum of 3c indicated signals at 4.33 ppm (-CH_2 peak), 5.87 ppm (-NH peak), and aromatic protons at 6.58 to 8.74 ppm, downfield -COOH at 10.60 ppm.

The IR spectrum of compound 3d showed NH at 3330 cm^{-1}, C=O at 1612 cm^{-1}, NO_2 at 1519 cm^{-1} and CH_2 at 1364 cm^{-1}. ^1H NMR of compound 3d indicated CH_2 as a singlet at 4.25 ppm, NH proton appeared as a singlet at 5.85 ppm, and aromatic protons were observed between 6.96 to 8.82 ppm. IR of 3e showed NH at 3365 cm^{-1}, C=O at 1610 cm^{-1}, C=N at 1576 cm^{-1}, aromatic C=C at 1504 cm^{-1}; C-N stretch 1393 cm^{-1}. ^1H NMR of 3e indicated CH_2 as a singlet at 5.08 ppm, -NH appeared as a singlet at 6.41 ppm and all aromatic protons were observed at 6.47-8.65 ppm. IR of 3f showed NH at 3464 cm^{-1}, C=O at 1611 cm^{-1}, C=N at 1595, aromatic ring breathing at 1490. CH_3 at 1355 cm^{-1}. ^1H NMR of 3f indicated CH_3 singlet at 3.31 ppm; CH_2 at 5.32 ppm, NH at 7.09 ppm, and aromatic protons at 6.8-8.6 ppm. IR spectrum of 3g showed NH at 3278 cm^{-1}, OH at 3500-3200 cm^{-1}. C=O at 1609 cm^{-1}, C=N at 1576 cm^{-1}, aromatic ring breathing at 1508.24 cm^{-1}. ^1H NMR of 3g indicated CH_2 singlet at 4.23 ppm, NH at 6.70 ppm, aromatic ring at 6.43-8.74 ppm, and OH proton at 9.98 ppm. 3a-g were further confirmed by molecular ion peaks of mass spectra analyses and elemental analyses.

Biological activity

The antibacterial activity of the novel compounds (1, 2, 3a – 3g) was assessed using the disc diffusion method at a concentration of 5 mM in DMSO (dimethyl sulfoxide) solvent [14]. The synthesized compounds were tested for their antibacterial activity against both Gram-positive bacteria, such as *Staphylococcus aureus MTCC 96* and *Bacillus subtilis MTCC 441*, and Gram-negative bacteria, including *Pseudomonas aeruginosa MTCC 1688* and *Escherichia coli MTCC 443*. The reference drug was penicillin g for antimicrobial activity.

The results of antimicrobial screening (Table 1) indicate that the synthesized compounds have a major influence on the antibacterial profile of *P. aeruginosa* and *E. coli* strains (Gram-negative bacteria). Compounds 2, 3a, and 3c showed significant antimicrobial activity against *Bacillus subtilis* as they contain -Cl, -NO_2 and -COOH groups. So, nitro and carboxylic acid groups at para-position enhance antimicrobial activity.

Table. 1. Antimicrobial activity screening result of synthesized compounds, Gram-negative and Gram-positive bacteria in inhibition zone diameter mm/5 mM.

Antibacterial activity				
Compound no.	Microorganisms and zone of inhibitor (mm/5 mM)			
	Gram-negative bacteria		Gram-positive bacteria	
	P. aeruginosa	*E. coli*	*S. aureus*	*B. subtilis*
1	11	19	12	12
2	17	22	17	27
3a	24	39	19	37
3b	29	24	22	22
3c	20	26	26	35
3d	26	24	24	22
3e	18	20	20	18
3f	24	26	17	22
3g	22	29	24	20
Penicillin-g	15	23	25	25

ADME Studies

Studies of ADME and toxicity were carried out for these compounds through Absorption, Distribution, Metabolism, and Excretion (ADME) which is a computational approach for assessing drug-likeness in the bloodstream. Each of these processes can be analyzed independently using specific methods [17]. For example, Lipinski, Ghose, Veber, Egan, Muegge, and the compound's bioavailability score are physiochemical characteristics that provide information on drug-likeness [15]. Based on Egan's multi-statistical graph model 44, the Brain or Intestinal Estimated Permeation makes use of polarity (TPSA) and lipophilicity (WlogP) to forecast CNS access and human intestine absorption (HIA) *via* a breach in the blood-brain barrier. Thus, the ellipse created by the polarity and lipophilicity profiles intersecting takes into account both strongly and poorly absorbed substances within a human intestine and follows a linear trend. Therefore, the majority populous area of compounds with high HIA, including WlogP values between 0.4 and 6.0 and TPSA lower than 79.2, is indicated by the ellipse created with TPSA less than 142.2 and WlogP between 2.3 and 6.8. The compound's portrayal as a boiled egg provides details about the anticipated Small-molecule penetration of the brain and absorption in the gastrointestinal tract [18]. The scores of all derivatives in the high gastrointestinal absorption (GIA) zone can be seen inside the radar plot of Figure 1, where WlogP values range from 2.62 to 4.09 and TPSA values from 49.57 to 112.32. As a result, all compounds which have the highest oral bioavailability score also have the lowest lipophilicity and polarity index making up the class of compounds with a high GIA.

Molecular docking

By using Autodock 1.5.7 the target enzyme amylase's (PDB: 1SA0) active site was docked for all of the synthesized variants in this series using molecular docking software [19]. Auto Dock Vina was used to calculate the binding energies of all benzimidazole derivatives, and all binding contacts generated at a distance of 5Å from the ligand were examined. A standard nocodazole (anti-neoplastic agent) was used for docking. When creating structure-based drug residue, molecular docking is a helpful technique [20]. Figure 2 presents the optimized structures of the three most effective benzimidazole-pyridines employed in the docking investigation. Our research sought to understand how the most potent analog molecules, 3e, 3f, and 3g, interacted with the various amino acids shown in Figure 2 in inappropriate (2D) and (3D) ways. Using energies of -8.1, -8.1, and -8.1 kcal mol^{-1}, respectively, Table 3 shows that compounds 3e, 3f, and 3g with strong inhibitory effects occupied acceptable places at the binding center of HPA.

Table 2: Estimated absorption and distribution characteristics, as well as anticipated "drug-like" qualities

Compound	Lipinski drug like						Veber drug like	Solubility	ABS	Absorption and distribution		
	Mol. wt.	MlogP	H-Bond Acceptors	H-Bond Donors	TPSA	Rotatable bonds	ESOL		WlogP	GI	P-gp	BBB
1	195.22	1.66	2	1	41.57	1	Soluble	0.55	2.62	High	Yes	Yes
2	271.7	2.34	3	0	47.78	3	Soluble	0.55	2.98	High	No	Yes
3a	373.36	1.49	5	1	105.63	6	Moderately soluble	0.55	4.09	High	No	No
3b	342.39	2.97	3	1	59.81	5	Moderately soluble	0.55	3.97	High	No	Yes
3c	372.38	0.99	5	2	97.11	6	Moderately soluble	0.56	3.36	High	No	No
3d	373.36	1.49	5	1	105.63	6	Moderately soluble	0.55	4.09	High	No	No
3e	328.37	2.75	3	1	59.81	5	Moderately soluble	0.55	3.66	High	No	Yes
3f	370.4	2.3	4	1	76.88	6	Moderately soluble	0.55	3.86	High	No	Yes
3g	344.37	1.93	4	2	80.04	5	Moderately soluble	0.55	3.37	High	No	No
Std Nocodazole	301.32	1.21	4	2	112.32	5	Soluble	0.55	2.84	High	No	No

Note: Mol. wt. - Molecular weight, MlogP- Topological method implemented, TPSA- Topological polar surface area, ESOL- Estimated aqueous solubility, WlogP- atomistic method implemented, GI- Gatrointestinal absorption, P-gp- P-glycoprotein substrate, BBB- Blood brain barrier parameter.

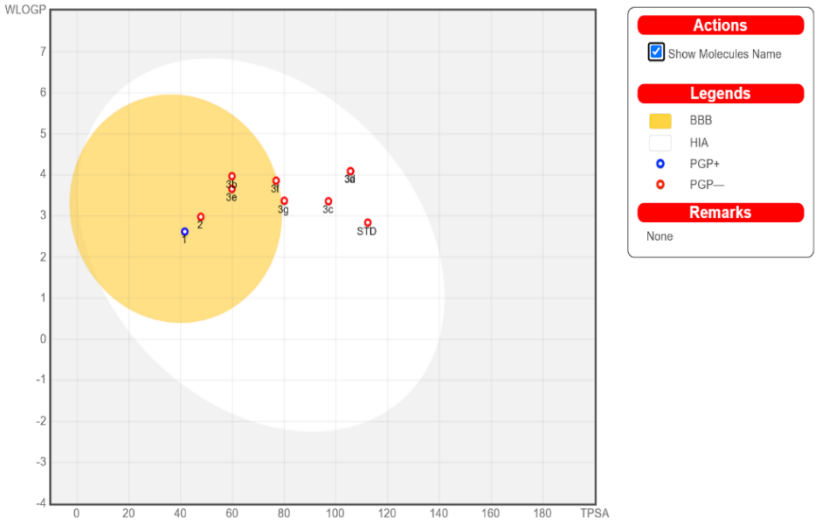

Figure 1. BOILED-Egg representation of benzimidazole-pyridine derivatives

Table 3: Complexes with 1SA0 docking binding energies (kcal.mol^{-1}).

Compounds	1SA0
1	-6.0
2	-6.6
3a	-7.5
3b	-7.7
3c	-7.6
3d	-7.8
3e	*-8.1*
3f	*-8.1*
3g	*-8.1*

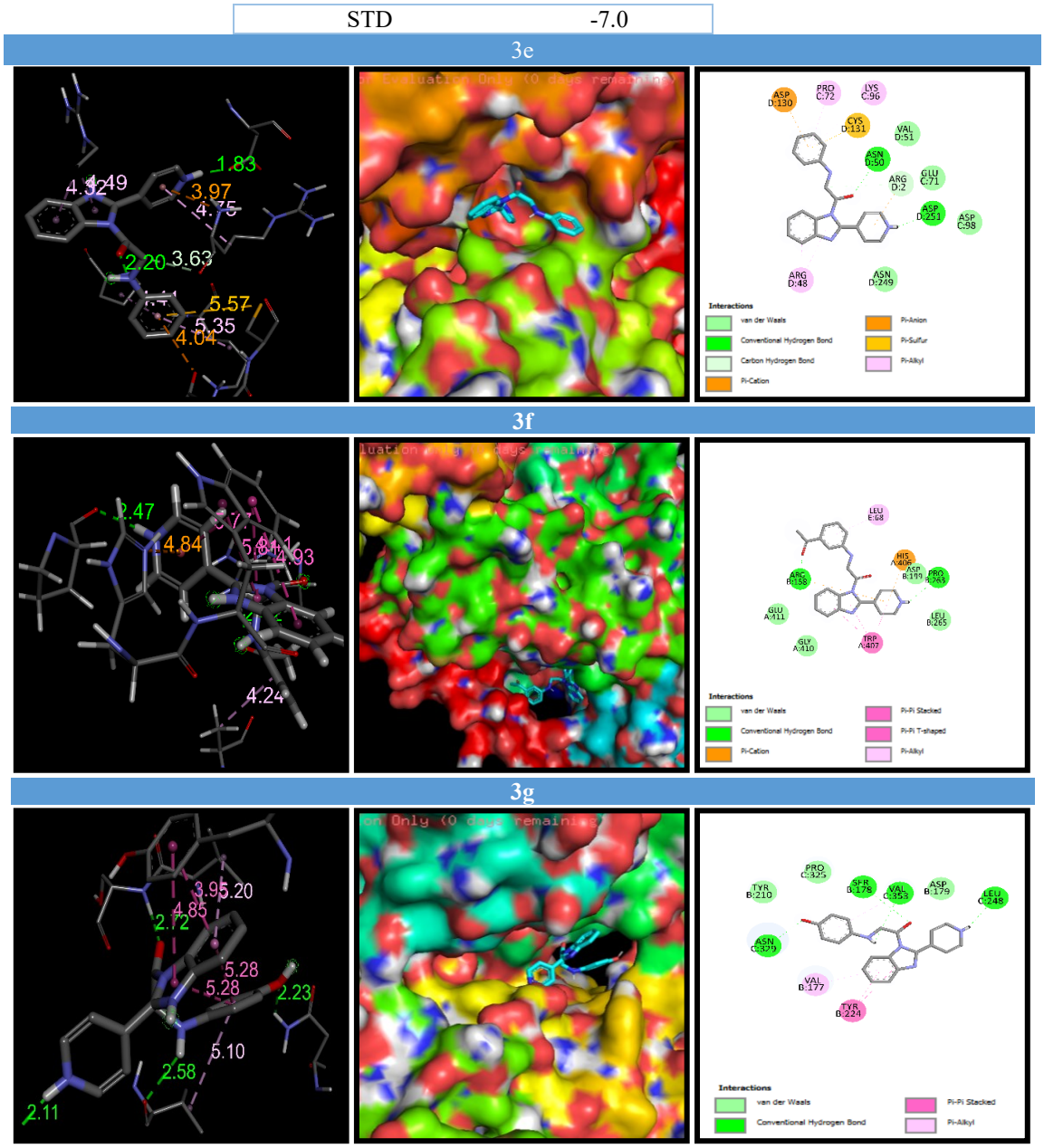

Figure 2. 3D binding distance, 3D surface intraction and 2D interaction of ligand and protein 1SA0.

Figure 2 shows the structure of the 3e given (π-anion) interaction with ASP D:130 (4.04Å), (π-alkyl) interaction with PRO D:72 (4.44 Å), (π-alkyl) interaction with CYS D:96 (5.35 Å), (π-sulfur) interaction with CYS D:131 (5.57 Å), one H-bond with VAL D:51 (3.63 Å), van der Waals interaction with VAL D:51 (3.63Å) two (π-alkyl), interaction with ARG D:48 (4.32 & 4.49 Å), one C-H bond with ARG D:2 (3.97 Å),(π-cation), interaction with ASN D:249 with (3.97), (π-alkyl) interaction with ARG D:2 (4.75 Å), and one H-bond with ASP D:251 (1.83 Å). And 3f shows the (π -alkyl) interaction with LEU E:68 (4.24 Å), one H-bond with ARG B: 158 (4.42 Å), (π -cation) interaction with HIS A:406 (4.84 Å), Three π-π stacked interaction with TRP A:407 (5.77 Å, 5.81 Å, 4.93 Å), and one H-bond with PRO B:263 (2.47 Å). And 3g shows the two (-alkyl) interaction with VAL B:177 (5.10, 5.20), one H-bond with LEU C:248 (2.11), two π-π stacked interaction with TYR B: 224 (5.28, 4.85), one H-bond with ASN C:329 (2.23), One H-bond with VAL C:353 (2.58), and one H-bond with SER B: 178 (2.72).

CONCLUSİON

Targeted benzimidazole pyridine fused analogs were synthesized by condensation of 2-chloro-1-(2-pyridin-4yl)-1H-benzo[d]imedazol-1-yl)ethan-1-one with different aromatic amines. Benzimidazole pyridine fused derivatives showed excellent antimicrobial potency with P. *aeruginosa*, *E. coli*, *S. aureus*, and *B. subtilis*. Insertion of -NO_2 and -COOH groups at para-position enhances

antimicrobial potency. A study on the chemicals' absorption, distribution, metabolism, and excretion (ADME) reveals good compatibility and no side effects on the central nervous system (CNS). ADME profiles are moderately water-soluble, blood-brain barrier (BBB) with non-permeant and high GIA absorbance. Molecular docking of the title compounds to tubulin showed that it binds to the colchicine site of tubulin with a binding mode compatible to that of nocodazole. Title compounds provide a promising range of opportunities for future lead optimization of drug development.

Acknowledgement: *Gratitude is extended to Dr. Devanshu Patel, the President of Parul University, for his generous provision of essential facilities.*

REFERENCES

1. C. Rao, N. Naidu, J. Priya, K. Rao, K. Ranjith, S. Shobha, B. Chowdary, S. Siddiraju, S. Yadam, *Biomedical Informatics*, **17**, 404 (2021). https://doi.org/10.6026/97320630017404
2. M. Andrzejewska, L. Yepez-Mulia, A. Tapia, R. Cedillo-Rivera, A. Laudy, B. Starościak, Z. Kazimierczuk, *European Journal of Pharmaceutical Sciences,* **21**, 323 (2004). http://doi.org/10.1016/ j.ejps.2003.10.024
3. K. Ansari, C. Lal, *European Journal of Medicinal Chemistry*, **44**, 4028 (2009). https://doi.org/ 10.1016/j.ejmech.2009.04.037
4. N. Phan, T. Huynh, H. Nguyen, Q. Le, N. Nguyen, K. Ngo, T. Nguyen, K. Ton, K. Thai, T. Hoang. *ACS Omega,* **8**, 28733 (2023). https://doi.org/10.1021/ acsomega.3c03530
5. E. Mulugeta, Y. Samuel, *Biochemistry Research International,* **13**, 1 (2022). https://doi.org/10.1155/ 2022/7255299
6. V. Grenda, R. Jones, G. George, M. Sletzin, *ACS Publication,* 30, 259 (1965). http://doi.org/10.1021/ jo01012a061
7. S. Thurston, G. Hite, A. Petry, R. Sidhartha. *Elsevier B.V.* **37**, 321 (2015). http://doi.org/10.1016/ bs.seda.2015.08.008
8. P. Zhan, C. Pannecouque, E. Clercq, X. Liu, *Journal of Medicinal Chemistry*, **59**, 2849 (2016). https://doi.org/10.1021/acs.jmedchem.5b00497
9. S. Hussain, M. Taha, F. Rahim, S. Hayat, K. Zaman, N. Iqbal, M. Selvaraj, M. Sajid , M. Bangesh, F. Khan, , K. Khan, N. Uddin, S. Shahi, M. Ali, *Journal of Molecular Structure*, **1232**, 1 (2021). https://doi.org/10.1016/ j.molstruc.2021.130029.
10. N. Thi, E. Pozioc, N. Van De, N. Praet, P. Pezzotti, S. Gabriel, M. Claes, N. Thuya, P. Dorny, *Acta Tropica,* **139**, 93 (2014). https://doi.org/10.1016/ j.actatropica.2014.07.012.
11. K. Ansari, C. Lal, *European Journal of Medicinal Chemistry*, **44**, 4028 (2009). https://doi.org/ 10.1016/j.ejmech.2009.04.037
12. L. Gatta, F. Perna, N. Figura, C. Ricci, J. Holton, L. D'Anna, M. Miglioli, D. Vaira, *J. Antimicrob. Chemother*., **51**, 439, (2003). doi:10.1093/jac/dkg085
13. Z. Ates-Alagöz, M. Alp, C. Kus, S. Yildiz, E. Buyukbingöl, H. Göker, *An International Journal Pharmaceutical and Medicinal Chemistry*, **339**(2), 74, (2006). https://doi.org/10.1002/ardp.200500168
14. M. Marinescu, C. V. Popa, *International Journal of Molecular Sciences*, **23**(10), 5659, (2022). https://doi.org/10.3390/ijms23105659
15. B. Srinivas, M. Subramanyam, G. K. Srinivasulu, K. Prabhakara Rao, Bulg. Chem. Commun., **53**(1), 10 (2021). https:// doi.org/10.34049/bcc.53.1.5165
16. A. Daina, O. Michielin, V. Zoete, *J. Chem. Inf. Model*., **54**, 3284 (2014). https://doi.org/10.1021/ ci500467k
17. M. Argirova, M. Guncheva, G. Momekov, E. Cherneva, R. Mihaylova, M. Rangelov, N. Todorova, P. Denev, K. Anichina, A. Mavrova, D. Yancheva, *Molecules*, **28**(1), 291 (2022). https://doi.org/ 10.3390/molecules28010291
18. M. Hay, D. Thomas, J. Craighead, C. Economides, J. *Rosenthal. Nature Biotechnology,* **32**, 40 (2014). https://doi.org/10.1038/nbt.2786
19. J. Silva, M. Rocha, E. Marinho, *J. Anal. Pharm. Res.,* **10**, 177 (2021). https://doi.org/10.15406/ japlr.2021.10.00384
20. L. Aroua, A. Alosaimi, F. Alminderej, S. Messaoudi, H. Mohammed, S. Almahmoud, S. Chigurupati, A. Albadri, N. Mekni, *Pharmaceutics*, **15**, 457 (2023). https://doi.org/10.3390/pharmaceutics15020457

Synthesis, biological evaluation, ADME studies and molecular docking with β-tubulin of fused benzimidazole-pyridine derivatives

D. Panchani[1], S. Maurya[1], T. Thaker[1]*, V. Rathod[1], Sh. Thakur[2]

[1]*Department of Chemistry, Parul Institute of Applied Sciences, Parul University, Waghodia, Vadodara-391760, Gujarat, India*

[2]*Department of Forensic Science, Parul Institute of Applied Sciences, Parul University, Waghodia, Vadodara-391760, Gujarat, India*

Table of contents

Spectral Data:

Compound 1:

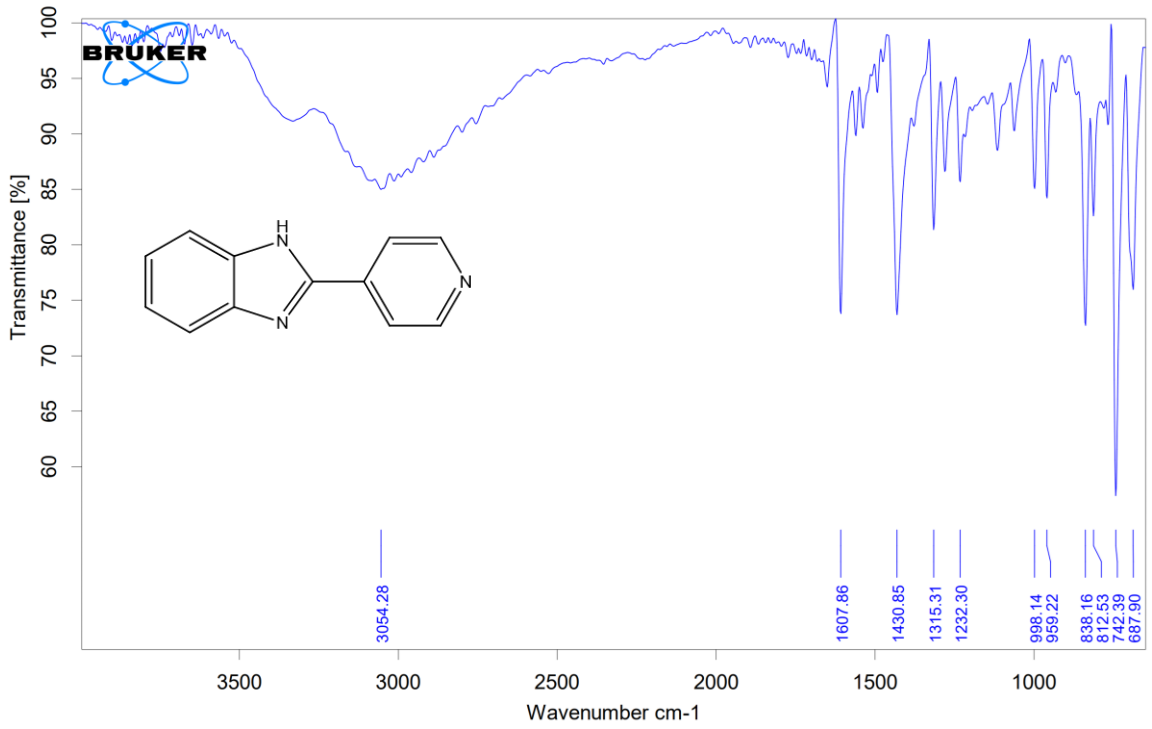

Figure S1: IR DATA of 2-(pyridin-4-yl)-1H-benzo[d]imidazole (1)

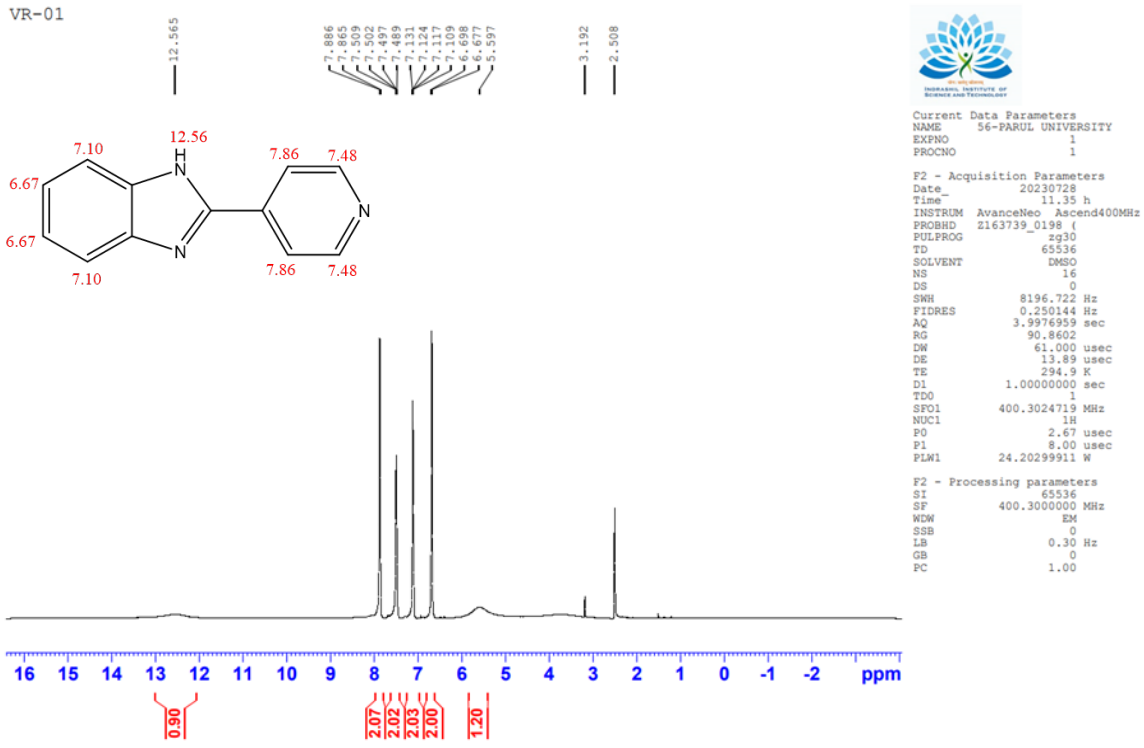

Figure S2: ^{1}H NMR DATA of 2-(pyridin-4-yl)-1H-benzo[d]imidazole (1)

Compound 2:

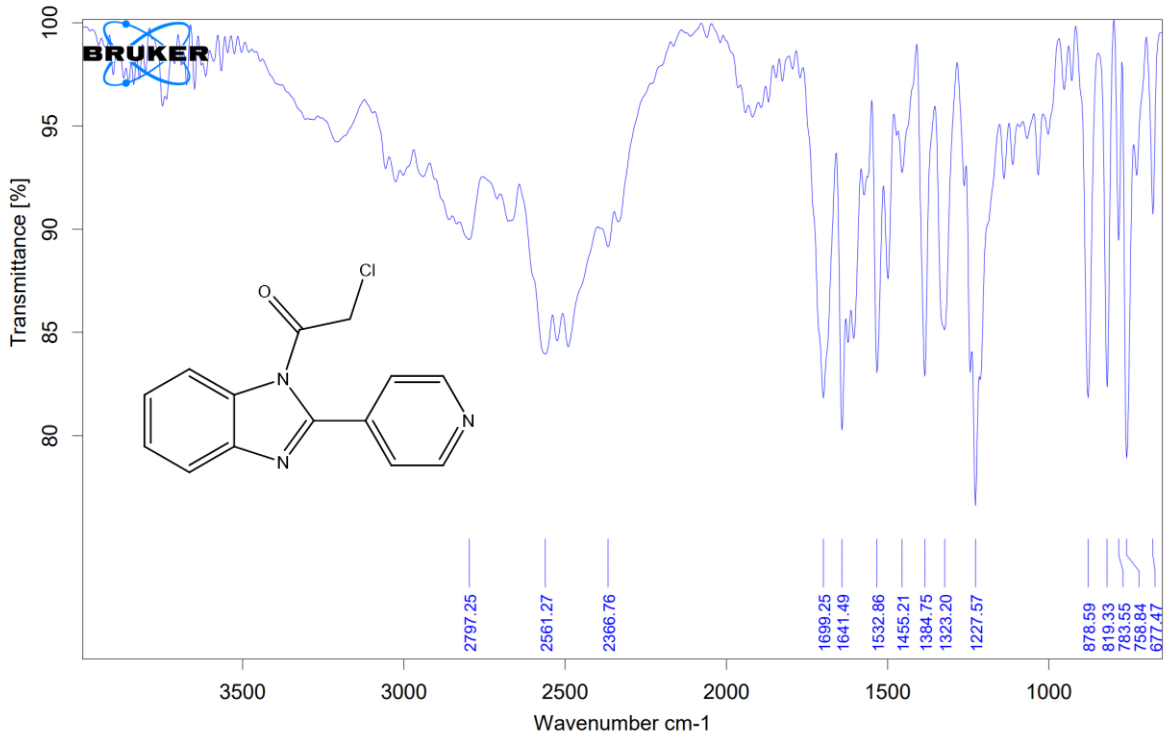

Figure S3: IR DATA of 2-chloro-1-(2-(pyridin-4-yl)-1H-benzo[d]imidazol-1-yl)ethan-1-one (2)

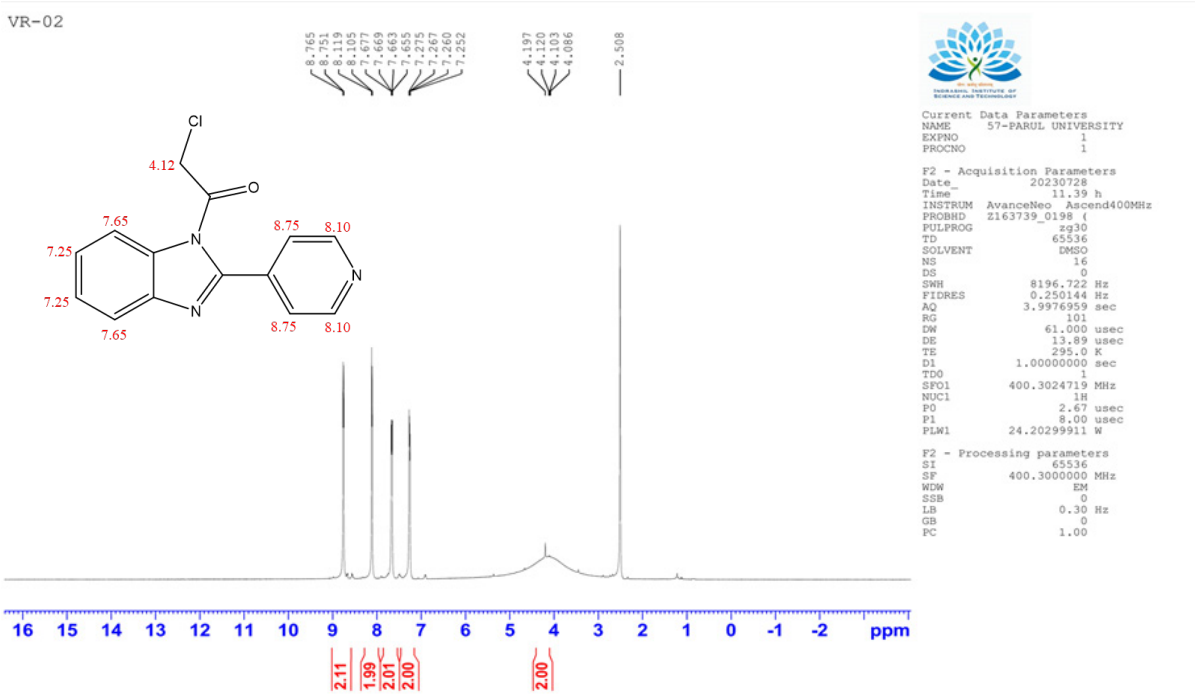

Figure S4: ^{1}H NMR DATA of 2-chloro-1-(2-(pyridin-4-yl)-1H-benzo[d]imidazol-1-yl)ethan-1-one (2)

Compound 3a

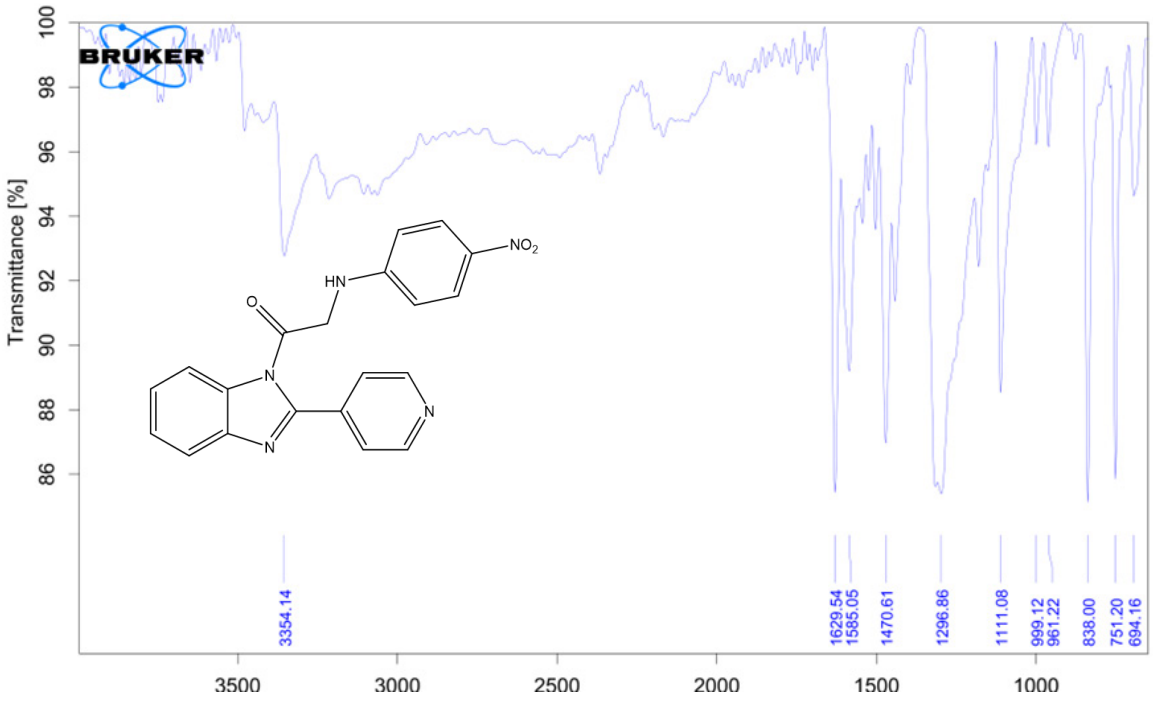

Figure S5: IR DATA of 2-((4-nitrophenyl)amino)-1-(2-(pyridin-4-yl)-1H-benzo[d]imidazol-1-yl)ethan-1-one (3a)

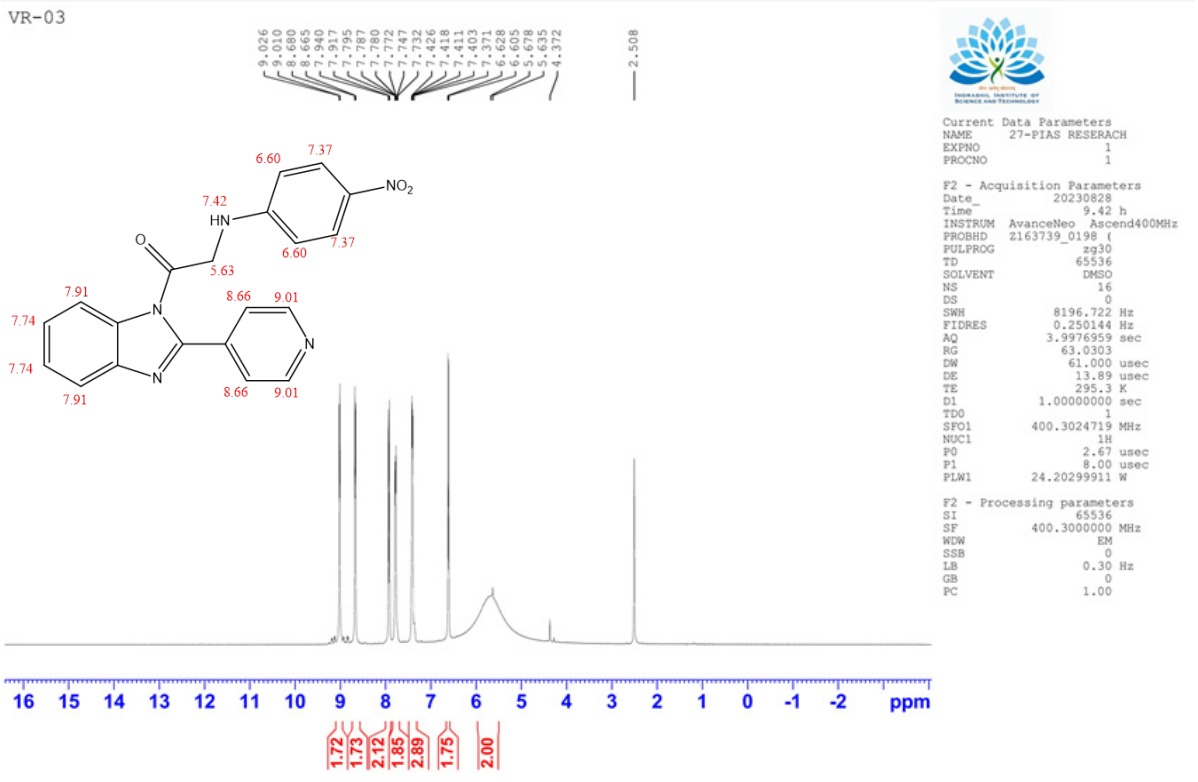

Figure S6: ^{1}H NMR DATA of 2-((4-nitrophenyl)amino)-1-(2-(pyridin-4-yl)-1H-benzo[d]imidazol-1-yl)ethan-1-one (3a)

Compound 3b

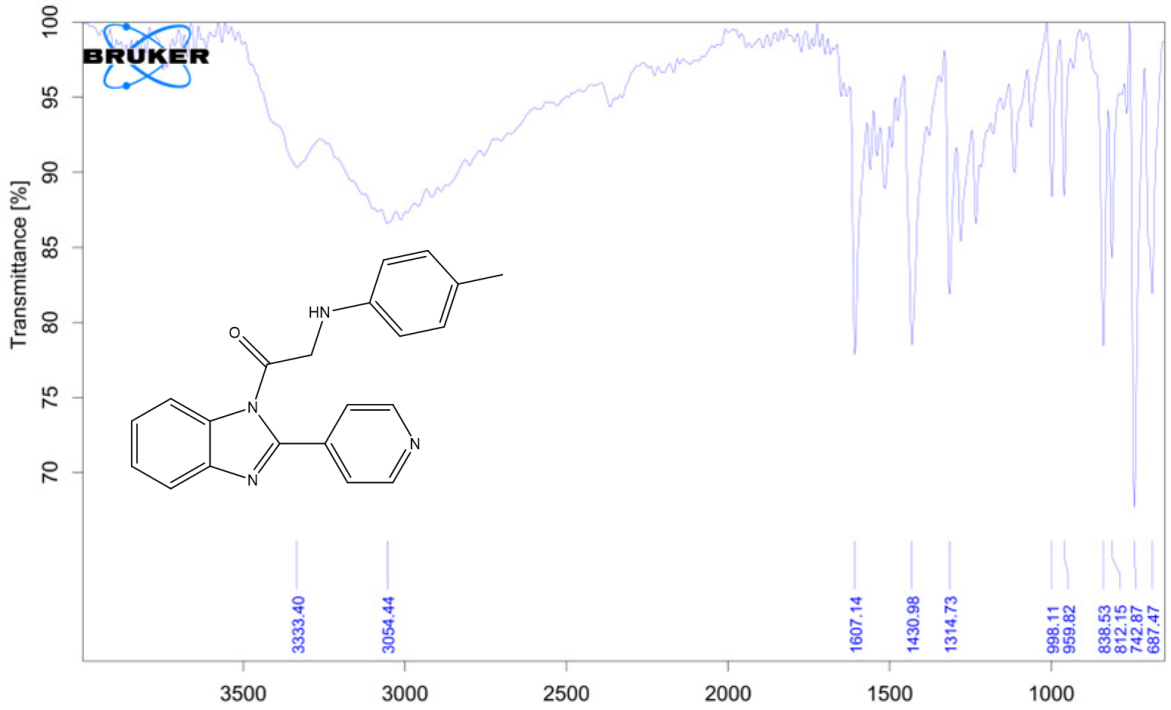

Figure S7: IR DATA of 1-(2-(pyridin-4-yl)-1H-benzo[d]imidazol-1-yl)-2-(p-tolylamino)ethan-1-one (3b)

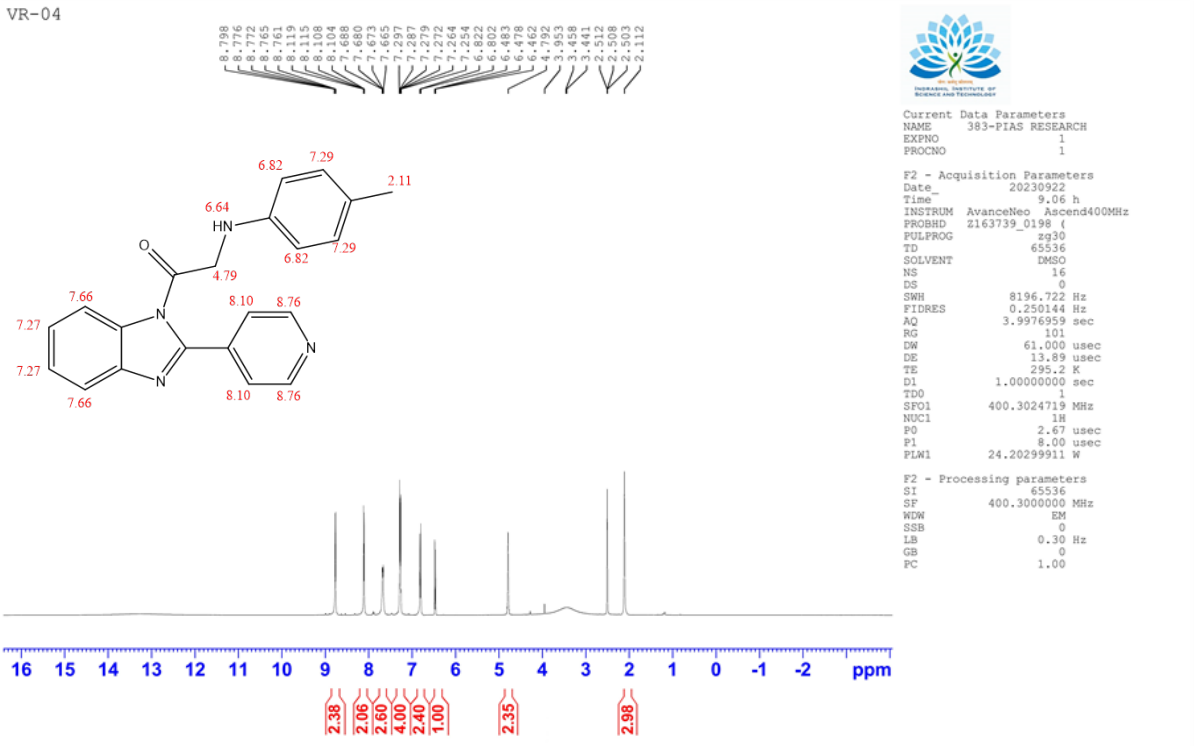

Figure S8: ^{1}H NMR DATA of 1-(2-(pyridin-4-yl)-1H-benzo[d]imidazol-1-yl)-2-(p-tolylamino)ethan-1-one (3b)

Compound 3c

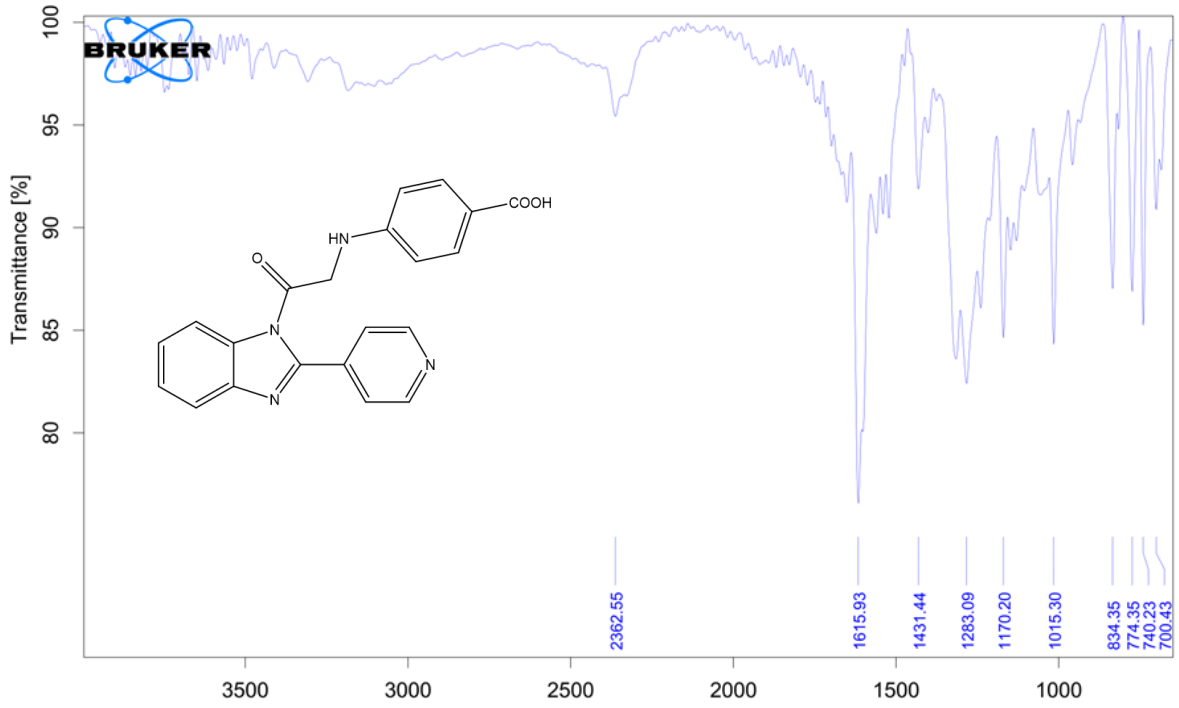

Figure S9: IR DATA of 4-((2-oxo-2-(2-(pyridin-4-yl)-1H-benzo[d]imidazol-1-yl)ethyl)amino) benzoic acid (3c)

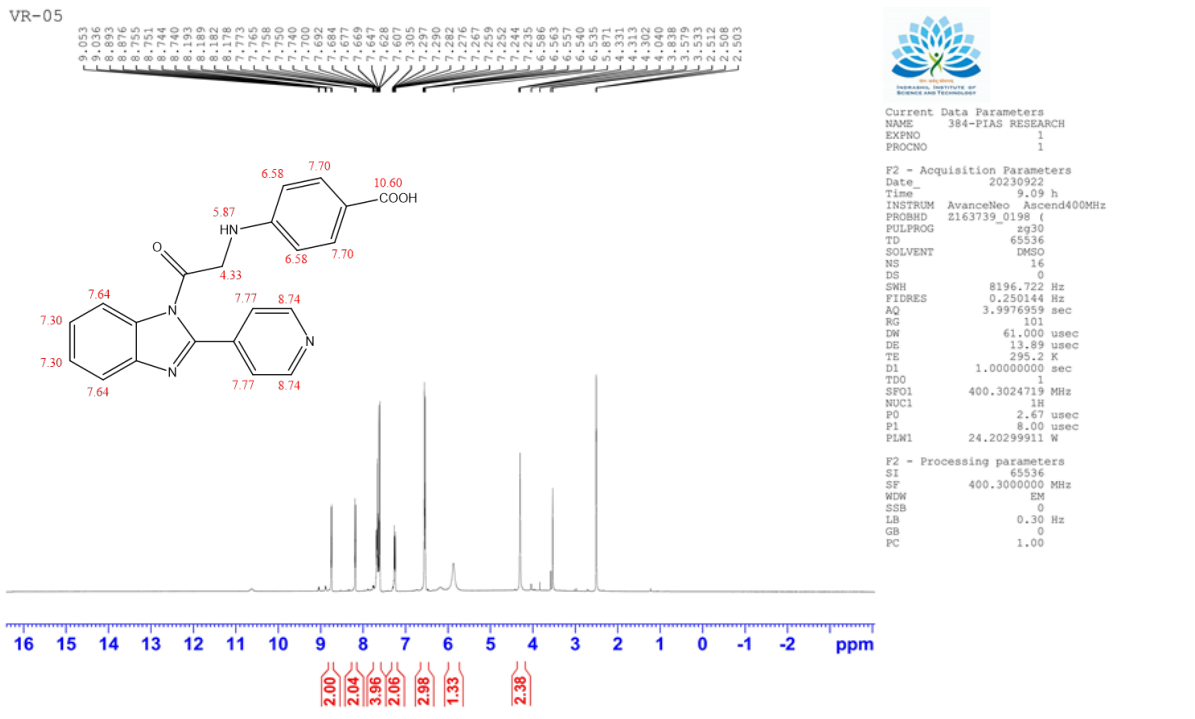

Figure S10: ^{1}H NMR DATA of 4-((2-oxo-2-(2-(pyridin-4-yl)-1H-benzo[d]imidazol-1-yl)ethyl)amino) benzoic acid (3c)

Compound 3d

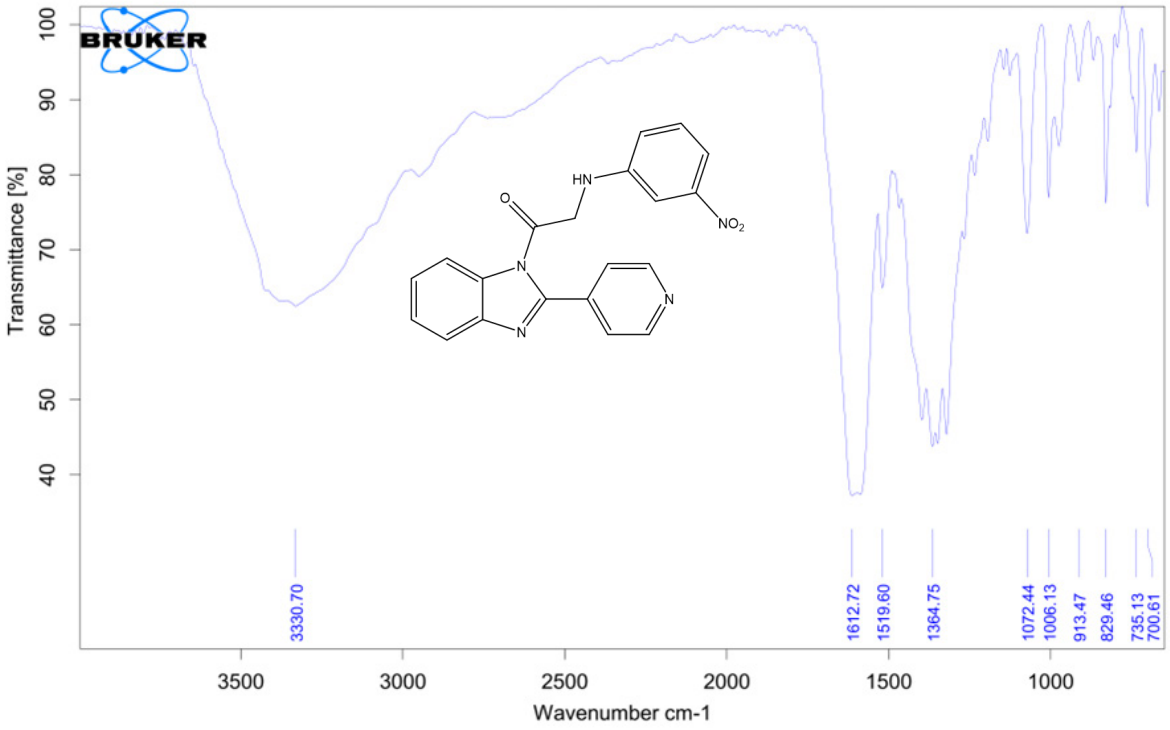

Figure S11: IR DATA of IR data of 2-((3-nitrophenyl)amino)-1-(2-(pyridin-4-yl)-1H-benzo[d]imidazol-1-yl)ethan-1-one (3d)

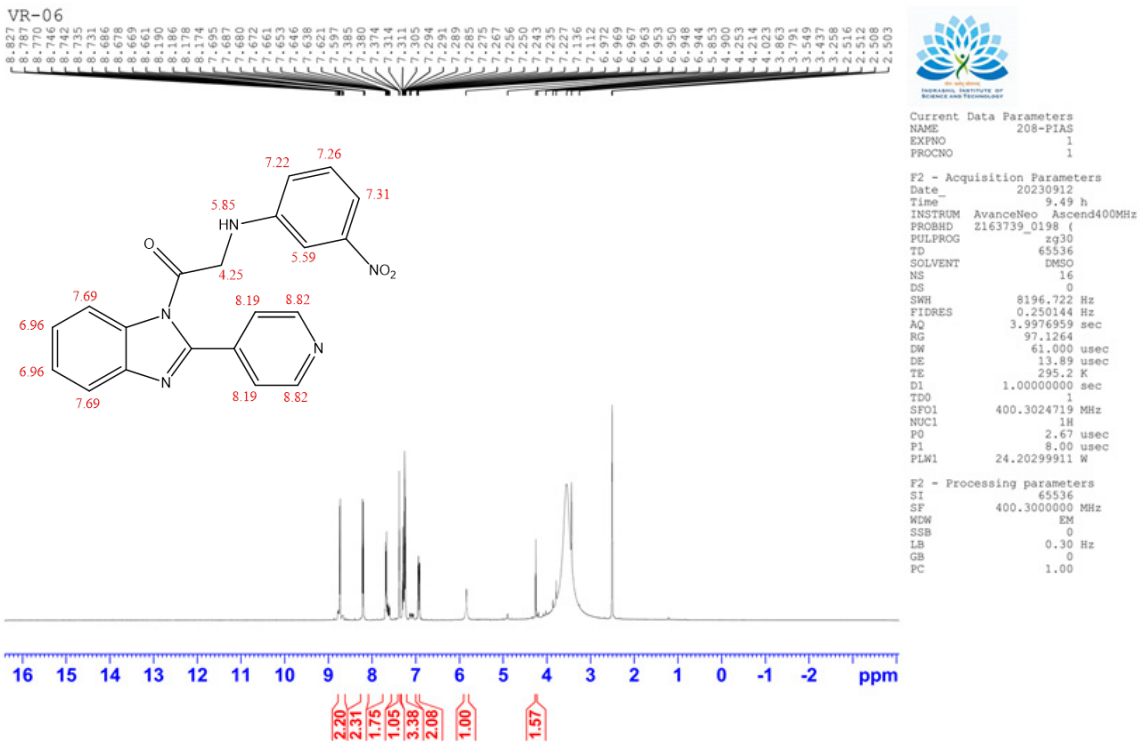

Figure S12: ^{1}H NMR DATA of IR data of 2-((3-nitrophenyl)amino)-1-(2-(pyridin-4-yl)-1H-benzo[d]imidazol-1-yl)ethan-1-one (3d)

Compound 3e

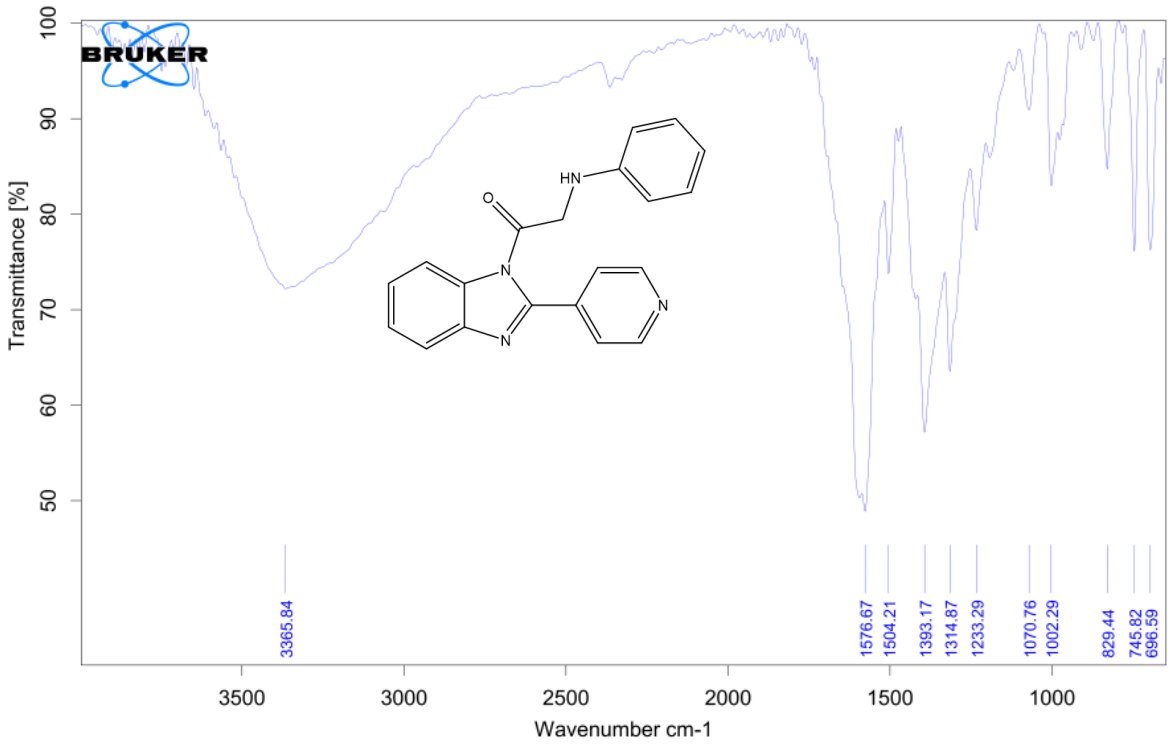

Figure S13: IR DATA of 2-(phenylamino)-1-(2-(pyridin-4-yl)-1H-benzo[d]imidazol-1-yl)ethan-1-one (3e)

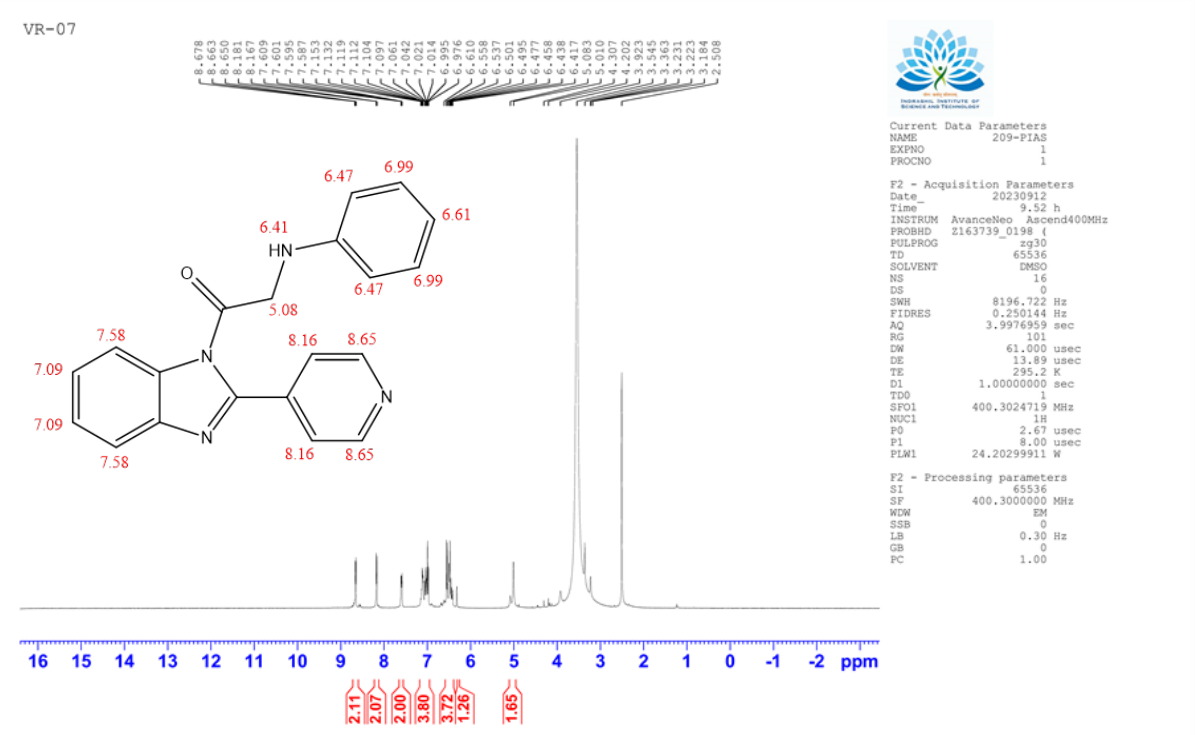

Figure S14: ^{1}H NMR DATA of 2-(phenylamino)-1-(2-(pyridin-4-yl)-1H-benzo[d]imidazol-1-yl)ethan-1-one (3e)

Compound 3f

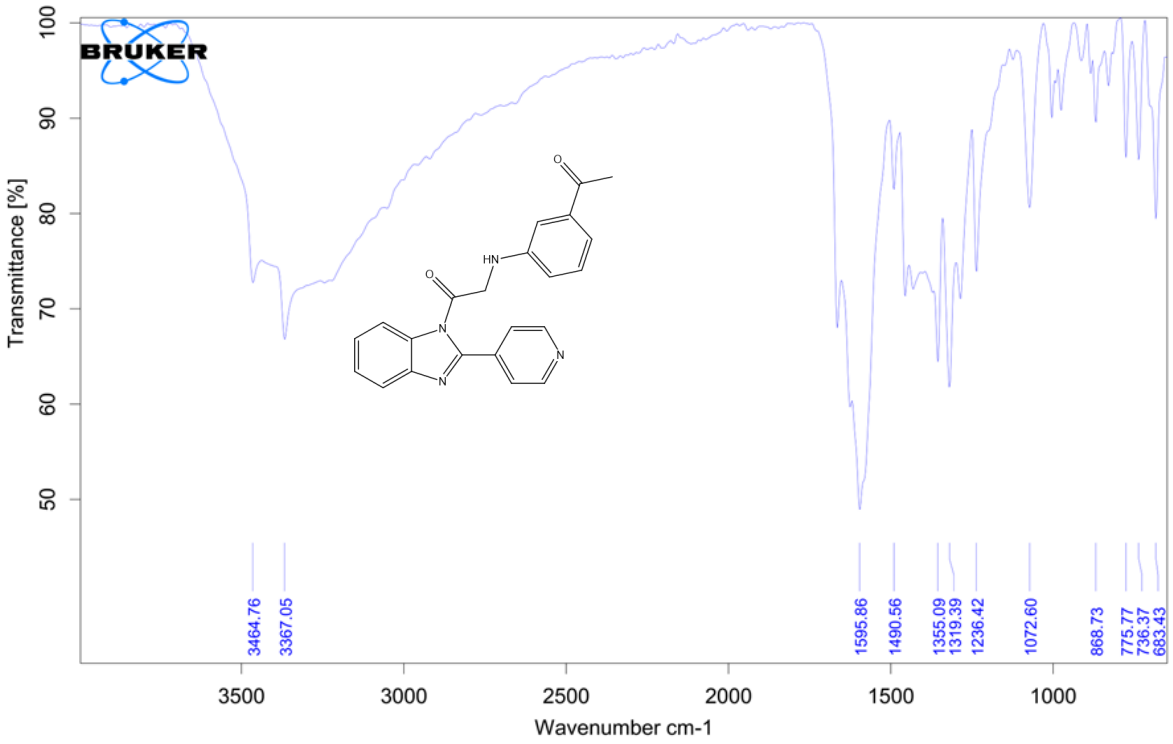

Figure S15: IR DATA of 2-((3-acetylphenyl)amino)-1-(2-(pyridin-4-yl)-1H-benzo[d]imidazol-1-yl)ethan-1-one (3f)

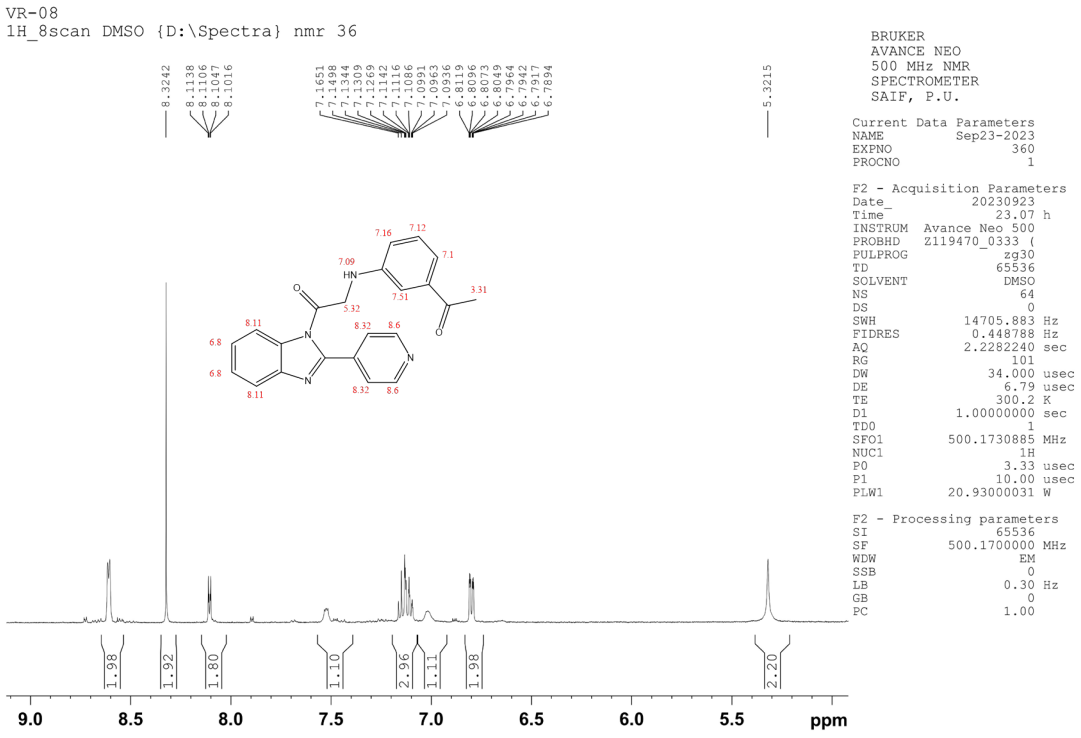

Figure S16: ^{1}H NMR DATA of 2-((3-acetylphenyl)amino)-1-(2-(pyridin-4-yl)-1H-benzo[d]imidazol-1-yl)ethan-1-one (3f)

Compound 3g

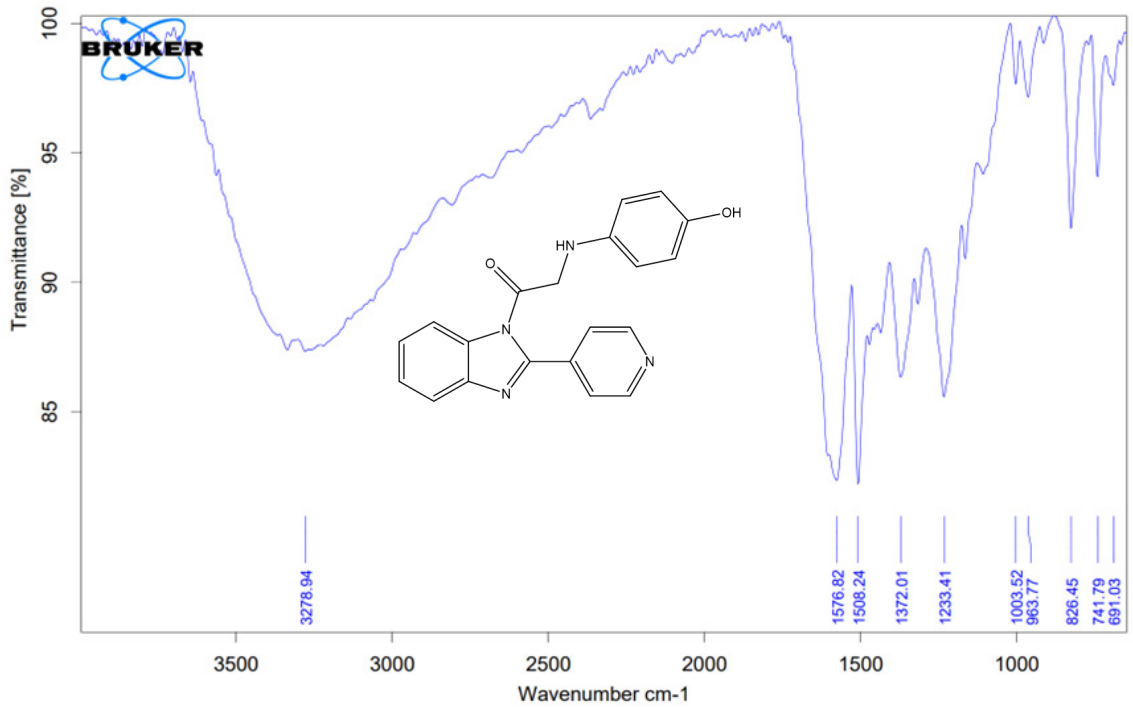

Figure S17: IR DATA of 2-((4-hydroxyphenyl)amino)-1-(2-(pyridin-4-yl)-1H-benzo[d]imidazol-1-yl)ethan-1-one (3g)